AIAA Guidance, Navigation, and Control Conference and Exhibit
5-8 August 2002, Monterey, California

AIAA 2002-4548

AIAA-2002

Active Failure Management for Aircraft Control Recovery

Sonja Glavaški, Michael Elgersma, Michael Dorneich, Peter Lommel

Honeywell Global Control Laboratory
Minneapolis, MN 55418
sonja.glavaski@honeywell.com

Abstract

This paper describes development and performance analysis of an active failure management system for the commuter and business aircraft control recovery. System failures are detected and isolated using a hierarchy of techniques that is chosen to ensure minimal disruption of operations and to minimize the number of false alarms. Successive layers in the diagnostics hierarchy are increasingly invasive. Higher layers will be invoked only when lower layers indicate a potential problem. Once a failure has been detected and identified, the failure can be accommodated in several ways, from passive pilot cueing to active autopilot reconfiguration. This paper also describes some preliminary pilot cueing strategies and displays to alert pilots to true failures, provide guidance on recommended responses, and inform the pilot of any reconfigurations. [1]

1. Introduction

To achieve safety goals in air travel proposed for the next decade, it will become necessary, among other measures, to actively deal with and recover from a large class of aircraft system failures. In general terms the class of problems that need to be addressed are common among the different segments of the air transport market. However, there are sufficient differences in the vehicles and their equipment, operations, and commercialization to justify studying the different segments of the markets separately. We develop and analyze performance of an active failure management for control recovery system for the commuter and business aircraft.

We focus on commuter aircraft for the regional airlines because commuter airline crashes are far more common than those for commercial transports. Reference [1] provides data on the circumstances and malfunctions associated with commuter airline crashes during the period 1983-1988. Study places the 118 crashes studied into 10 mutually exclusive categories. Of these, the largest numbers of cases cited were due to mechanical failure during climb-out, cruise, and approach (20) and to loss of control on takeoff/landing (22). Although aircraft icing falls somewhat lower on the list above, we include it here because we believe it too is amenable to advanced control solutions.

We address detection, isolation, and accommodation of selected mechanical failures as well as aircraft icing. Such failures will be uncovered by failure detection and system parameter identification and dealt with using a combination of pilot cueing, and autopilot reconfiguration wherever feasible.

We select the class of jet aircraft to be examined along with a general model representative for that class suitable for simulation studies. We define several candidate failure scenarios (e.g., aircraft icing, failures of control surface actuators, stuck or floating control surfaces, etc.) that are both common occurrences and amenable to improved control solutions. In this paper we develop detection algorithm and an algorithm that allows the rapid on-board identification of the parameters associated with a six-degree-of-freedom nonlinear model of an aircraft and parameters associated with individual actuators.

The parameter ID uses time-domain signals, but initial parameter estimates can also be obtained from linearizations of the nonlinear system about several operating points. For the time-domain parameter ID, we assume that we can measure all control inputs and states, and that the

[1] This research has been conducted under cooperative agreement #NCC-1-334 with NASA Langley Research Center and task order #1003 under contract NAS1-00107 with NASA Langley Research Center

state derivatives can be computed from the state values (see later section). Noise at the input (e.g. wind gust) affects the measured state and actual state in the same way, so it can act as additional excitation which can actually help parameter estimation. Noise at the output (e.g. unmodeled dynamics) affects the measured state but not the actual state, so output noise leads to errors in the parameter estimates.

We are currently developing autopilot reconfiguration algorithms to accommodate failures wherever possible and to provide pilot cueing to inform the pilot of the current situation, potential responses, and any autopilot reconfiguration. Performance is determined by simulations of the failure detection and system parameter identification algorithms, and autopilot reconfigurations under the defined failure scenarios.

2. Previous Work

References [3, 15, 14] describe many of the techniques which we use in the current paper. They describe both the parameter identification algorithms and their application to aircraft. They also describe various other algorithms and consider the trade off between using recursive least squares v.s. using a batch algorithm on a moving window of data. They also discuss the issues associated with turning off the identification when insufficient excitation is present, and effects of damage occurring (parameters value jumps) somewhere inside a window of data. Standard results for linear least squares problems can be found in [5] and [6]. Reference [7] contains many standard results in linear system identification.

Control surface effectiveness degradation due to icing has been extensively investigated [9, 8]. Reference [8] describes parameter identification for on-flight detection of aircraft icing.

Reference [10] presents a general methodology for adaptive control using multiple models, switching and tuning. This method allows a controller to operate in multiple environments by recognizing which environment is currently in existence and servicing it appropriately. The concept of using multiple models for switching or tuning is not new in control theory. Multiple model Kalman filters were studied in the 1970's. In this paper we present a practical applicatiom of active aircraft failure management system whose adaption is based on on-board aircraft aerodynamic parameter identification. This method allows for the pilot cueing strategies to deal with such failures, and for control reconfiguration strategies to prevent a failed vehicle from entering an extreme flight condition whenever possible.

3. Active Failure Management

System failures are detected and isolated using a hierarchy of techniques that is chosen to ensure minimal disruption of operations and to minimize the number of false alarms. Successive layers in the hierarchy are increasingly invasive. Higher layers will be invoked only when lower layers indicate a potential problem.

3.1. Failure Detection

Failure detection defines the first layer in hierarchy. It operates full time and requires no external test signals and includes its own hierarchy of methods.

Hardware-based failure monitors provide the first line of defense in failure detection. Commuter aircraft today have failure monitors covering various health aspects of the engine, hydraulics, auxiliary power, sensors, actuators, control surfaces, etc. These monitors are particularly useful for isolating simple problems: stuck actuator, surface hard overs, etc. But they are prone to common mode failures that set off multiple alarms simultaneously and contribute to pilot confusion. Many commuter aircraft also have sensors to detect icing, but these too are not always reliable. Thus, we will augment them with other methods.

Model-Based failure detection algorithms provide the next line of defense and are based upon simple comparisons of true aircraft responses to those of an internal model. Parameters for this internal model will be determined using system identification.

3.2. Failure Isolation

Failure detection in our terminology indicates only a potential failure. We rely on system parameter identification, which defines the next two layers in a hierarchy to both confirm that a failure has occurred and to isolate that failure to a particular element. Reliable system identification requires the use of test signals to excite the system to be identified. Occasional pilot inputs and scheduled autopilot maneuvers do provide useful test signals for identification, but they are relatively infrequent during much of the flight. When the failure detection algorithm indicates a potential failure, it will usually be necessary to inject a test signal to confirm this possibility and isolate the failure. We use classical detection theory methods to strike an acceptable balance between

false alarms (detecting a failure where none exists) and misses (not detecting a failure where one exists). Preliminary results will be presented later in the paper.

To minimize disruption to operations, we will first inject test signals into the null space of the inputs using redundant control surfaces such that these signals (ideally) cancel one another and thereby do not excite aircraft motion. This allows detection of failures among redundant control surfaces, where available, and is particularly useful for identifying changes in surface effectiveness. Where redundancy does not exist, we will use more general test signals that do excite aircraft motion. In general, test signals must be large enough so as not to be dominated by sensor noise and disturbances (i.e., gust inputs). On the other hand control inputs can not be too large since injecting test signals into the null space of the inputs using redundant control surfaces could be hazardous in the presence of actual failures. This is because the null space is no longer what it was before the failure. These general test signals should produce relatively small accelerations and need only last for a few seconds and even then only when failure detection indicates a potential problem.

3.3. Control Recovery

To accommodate failures wherever possible autopilot reconfiguration algorithms and pilot cueing strategy have to be developed. Pilot cueing is necessary to inform the pilot of the current situation, potential responses, and any autopilot reconfiguration. Control recovery will allow real-time in-flight updates to the aircraft autopilot in the face of confirmed and isolated failures. As such it is a potential alternative primarily for newly designed aircraft or for retrofit aircraft that are scheduled for flight control upgrades. Improved pilot cueing is the more likely option for the older retrofit market. Nevertheless, autopilot reconfiguration will be considered and will likely play a critical role in failures for which control bandwidth exceeds pilot capabilities (e.g., yaw damper). Autopilot reconfiguration consists of two steps: control reallocation and control reconfiguration.

For some types of failures, reconfiguration may be as simple as replacing one failed control surface with another similar surface and possibly making minor gain adjustments (e.g, split surface, where one half fails). In other cases, it may require replacing a failed surface with dissimilar surfaces, which could require recomputing the entire control allocation matrix. In yet more extreme cases (e.g., loss of hydraulics), it may require augmenting traditional control inputs with very non-traditional ones. We refer to all of the mentioned strategies as control reallocation.

4. Parameter Identification

Given a nonlinear dynamical system represented by a system of ordinary differential equations, with states x and inputs u:

$$\dot{x} = f(x,u)$$

our goal is to identify unknown parameters in the function f. To simplify the identification process, we can make use of the fact that if f has certain smoothness properties, then f can be approximated arbitrarily well by a nominal value, $f_{nom}(x,u)$, plus a linear combination of nonlinear basis functions, $b(x,u)$, where the coefficients in the linear combination form the unknown parameter matrix, H.:

$$\begin{aligned} \dot{x} &= f(x,u) \\ &= f_{nom}(x,u) + H * b(x,u) + \zeta \\ y &= C\ x + \eta, \end{aligned} \tag{1}$$

where

$$\begin{gathered} x \in R^n \quad y \in R^p \quad u \in R^m \quad b \in R^q \quad f \in R^n \\ H \in R^{n \times q} \quad C \in R^{p \times n} \quad p \leq n \end{gathered} \tag{2}$$

and ζ and η denote residual and measurement noise, respectively.

If only some rows of $f(x,u)$ depend on uknown parameters, then the parameter matrix H can be factored into a known matrix, g_x, times a smaller unknown coefficient matrix, H_x.

$$H = g_x * H_x$$

$$H_x \in R^{n_1 \times q} \quad g_x \in R^{n \times n_1}$$

The size of $||\zeta||$ decreases as the number of basis functions increases. As the number of basis functions increase, the number of columns of the coefficient matrices, H and H_x, also increases. Knowledge of the physics of the problem allows the choice of a small number of nonlinear basis functions that still give adequately small residual. After the basis functions have been chosen, the value of the coefficient matrix, H, must be determined. This can be done using either of two methods:

1) Using multiple linearizations

2) Using time domain data

The first method is used to initialize the parameters when several linearizations are available. The second method is used to refine the parameters using flight data, and can also be used to update the parameters after a failure has occured.

Both methods lead to a linear matrix equation for H of the form: $F = C * H * G$, with solution: $C * H = F * G^T * (G * G^T)^{-1}$.

If the matrix C is chosen so that $C\ g_x = I$, then $C * H = C * g_x * H_x = H_x$, so $F = (CH)G = H_x * G$ with solution: $H_x = FG^T * (GG^T)^{-1}$. When the G matrix is not full column rank, then a matrix, D, can be used to select only the columns of G that matter.

4.1. Parameter ID using Linearizations

Before using time-domain data to update the parameter matrix, H, it is often possible to get initial parameter estiamtes from linearizations of the full nonlinear simulation represented by $f(x,u)$. Linearization of the original system, about trim point i, gives: $\dot{x} = f(x_{0i}, u_{0i}) + [A,B]_i[x \quad x_{0i}, u \quad u_{0i}]$. Linearization of the parameterized approximation of the system gives: $\dot{x} = [f_{nom}(x_{0i}, u_{0i}) + H * b_{nom}(x_{0i}, u_{0i})] + [\partial f_{nom}/\partial[x,u] + H\partial b/\partial[x,u]][x \quad x_{0i}, u \quad u_{0i}]$

Setting the right-had sides of the above linearizations equal to each other, gives two sets of linear equations for the constant H matrix:

$$f(x_{0i}, u_{0i}) = f_{nom}(x_{0i}, u_{0i}) + H * b(x_{0i}, u_{0i})$$

$$[A,B]_i = [\partial f_{nom}/\partial[x,u] + H\ \partial b/\partial[x,u]]|_{(x_{0i},u_{0i})}$$

which can be combined to form: $F = (CH)G$, where $F = [F_1, F_2, ..., F_k]$ and $G = [G_1, G_2, ..., G_k]$ with entries given by:

$F_i = C_i[f(x_{0i}, u_{0i}) \quad f_{nom}(x_{0i}, u_{0i}),\ [A,B]_i \frac{\partial f_{nom}}{\partial[x,u]}|_{(x_{0i},u_{0i})}]D_i$

$G_i = [b(x_{0i}, u_{0i}), \{\partial b/\partial[x,u]\}|_{(x_{0i},u_{0i})}]D_i$

4.2. Time Domain Identification

After obtaining initial estimates for the parameter matrix, H, as described in the previous section, time domain data can be used to refine the parameter estimates. Time domain data can also be used to update the parameters after a failure has changed the values of the parameters.

For our aircraft model, we represent the aero forces and moments with the $H_x * b(x,u)$ term, while all other terms of the dynamics may be put into $f_{nom}(x,u)$. This is because minor failure of the aircraft can significantly change the aero coefficients, while having only a small effect on the mass and moment coefficients in $f_nom(x,u)$ and g_x.

If the aero coefficients themselves are considered as nonlinear functions of the state, those nominal nonlinear functions could either be put into the $f_{nom}(x,u)$ function, or H_x could be considered as a nominal nonlinear function plus a linear perturbation to be estimated. $H_x(x,u) = H_{x0}(x,u) + \Delta H_x$. Noise on the states can cause the nominal nonlinear table lookup values $f_{nom}(x,u)$ and $H_{x0}(x,u)$ to be noisy, therefore the states should be filtered before being used in those functions. It is assumed that x and u can be measured with sensors. Then by comparing the differentiated value of the measured x with the computed values of $f_{nom}(x,u)$ and $b(x,u)$, the coefficient matrix H_x can be computed.

The least-squares procedure for determining the parameter matrix acts to average out any high frequency noise introduced by differentiation of the noisy state. One concern is that the noise can cause biases in some cases, so any amplification of the noise due to differentiation of the state could increase the size of the bias. It has been shown in [4] that if $b(x,u) = u$ and there is no noise on u, then the least squares parameter solution will not be biased.

After acquiring k samples, let

$$\begin{aligned} F_k &= C\ [\dot{x}(t_1) \quad f_{nom}(x(t_1), u(t_1)), ..., \\ &\quad\ \dot{x}(t_k) \quad f_{nom}(x(t_k), u(t_k))] \\ G_k &= [b(x(t_1), u(t_1)), ..., b(x(t_k), u(t_k))] \\ C * H &= C * g_x * H_x = H_x = H_{x0} + \Delta H_x \end{aligned}$$

The G_k matrix is size $q \times k$ where $k \gg q$, so we have an over-determined linear algebra problem to solve for H_x.

$$F_k = H_x G_k = (H_{x0} + \Delta H_x) G_k$$

We may have some a-priori knowledge of what the value of the H_x matrix should be. In this case, we can bias the computed answer to stay close to the preferred value H_{x0}.

The unweighted least squares problem, can be weighted with a $q \times q$ weighting matrix W to keep ΔH_x small. This can be done as follows:

$$[0, F_k \quad H_{x0} G_k] = \Delta H_x [W, G_k]$$

Let σ_1 be the largest singular value of the $q \times k$ matrix G. Then a quantitative estimate on how much the size of $||\Delta H_x(W)||_2$ is reduced by the presence of the weighting matrix W is given by: $||\Delta H_x(W)|| \leq ||\Delta H_x(0)|| \frac{{\sigma_1}^2}{w^2 + {\sigma_1}^2} \leq ||\Delta H_x(0)||$.

Define the inverse covariance matrix $P_k^{-1} = ([W, G_k][W, G_k]^T)^{-1}$, so $P_0^{-1} = (WW^T)^{-1}$ and and define $\Delta H_{x0} = 0$

The iterative update for the $n \times q$ parameter matrix update is given by:

$$\Delta H_{xk+1} = \Delta H_{xk} + \frac{[C(\dot{x}_{k+1} \quad f_{nom\,k+1}) \quad H_{x0} b_{k+1}] b_{k+1}^T P_k^{-1}}{\lambda + b_{k+1}^T P_k^{-1} b_{k+1}}$$

while the inverse covariance matrix update is:

$$P_{k+1}^{-1} = [P_k^{-1} \quad \frac{P_k^{-1} b_{k+1} b_{k+1}^T P_k^{-1}}{\lambda + b_{k+1}^T P_k^{-1} b_{k+1}}]/\lambda$$

where $0 < \lambda \leq 1$ is a forgetting factor on the old data which replaces data that is i samples old with λ^i times that old data.

Once we have a solution for ΔH_{xk}, we can obtain $(\Delta H)_k = g_x \ \Delta H_{xk}$

In order to obtain a well-conditioned identification computation, it is necessary to have sufficient excitation, either from pilot maneuvers or external signal injection (e.g. sinusoids, square waves, or random noise).

When there are redundant actuators, then signals can be injected into the kernel of $\partial f(x,u)/\partial u$ without affecting $\dot{x}$. This type of injection can be used to identify the additional terms in $\partial f(x,u)/\partial u$ that are not identifiable from aircraft maneuvers alone.

The external signal generator is only turned on when the failure detection flag signal has exceeded some threshold size. This prevents excessive actuator wear, and avoids annoying the pilot. The pilot can see the surfaces moving when signals are being injected, and if the kernel of $\partial f(x,u)/\partial u$ is not accurately computed, the injected signals could have some affect on $\dot{x}$, which the pilot would feel. If the batch least-squares solution is used this time interval is fixed, but with the iterative solution, the parameter identification can be turned off whenever the error has decreased below some threshold value.

5. Pilot Cueing

A preliminary design of a cueing system for a hierarchy of active flight management techniques is presented in this paper. The automation in the system for active management of aircraft system failures, both active and passive, is responsible for detecting, isolating, and potentially compensating for upset conditions. It is vital that the pilots be aware of the automation as the automation manages faults. Thus, among the preliminary designs introduced in this paper, a dedicated display is necessary to support the pilot's awareness of the automation as it performs its tasks.

The full set of displays in the pilot cueing system is derived from a framework [DR00] of information requirements that addresses situation awareness by explicitly representing the automation as an agent that performs fault management tasks (detect, diagnose, prognose, and compensate) in the operational environment (either environment, system, aircraft, or mission). Given a prioritization and categorization scheme, alerts are realized on multiple displays including aural alerts, visual cues and symbology on existing flight displays, dedicated messages, and finally a dedicated situation awareness display.

Figure 1 illustrates a conceptual design of a Control Upset Automation Situation Awareness (CUASA) display. There are three primary components: (1) the primary flight control surface display, which depicts the control surface displacement within the scale of its (possible revised) limits, (2) the control authority display, which conveys to the pilot what the new limits (placed on the control inputs by the automation's reconfiguration) are on the three degrees of freedom: roll, pitch, and yaw, and (3) the message area, where dedicated messages alerting the pilot to automation-related tasks are presented.

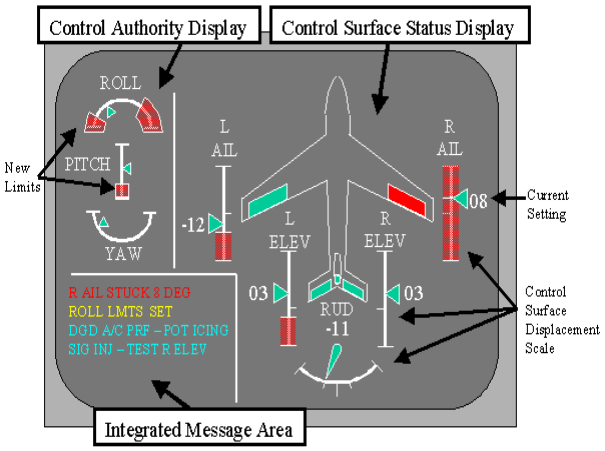

Figure 1: Integrated Message Area and Situation Awareness Display

6. Control Reconfiguration

In-flight system parameter identification ultimately provides the potential for in-flight control law reconfiguration. We address robustness to identification errors by limiting authority of pa-

rameter corrections derived from system identification.

The controller is parameterized with the coefficients in the H matrix, provided by the parameter identification algorithm. The controller starts out with the nominal value of the parameters, and is updated continuously with the current estimate of the parameter values. The dynamic inversion controller uses the plant model given in Section 7.1. Let $f_0(x) = f(H_x, x, 0)$ and $G_0(x) = \frac{\partial f(H_x,x,0)}{\partial u}$.

The desired dynamics are of the form:

$$\dot{x} = A(x \quad x_{cmd}), \qquad x_{cmd} = T * c_v$$

where $T \in R^{n \times m}$ and $c_v \in R^m$ are the m external command inputs.

With $u \in R^m$, m outputs can be controlled with these m inputs. Let $C \in R^{m \times n}$ be a matrix that selects which combinations of the state will be controlled. Then, the portions of the desired dynamics that can be obtained are:

$$C\dot{x} = CA(x \quad T * c_v)$$

Setting the right hand side of this equal to the right hand side of:

$$C\dot{x} = C\ f_0(x) + C\ G_0(x) * u$$

Gives:

$$CA(x \quad T * c_v) = C\ f_0(x) + C\ G_0(x)u$$

Solving for u gives the controller as a function of x and the external input, c_v:

$$u = (C\ G_0(x))\ {}^1C[A(x \quad Tc_v) \quad f_0(x)]$$

7. Simulation Results

Model-based monitoring and diagnosis of a physical system requires well-constrained dynamical models of the system. The ability to generate models that accurately describe dynamics of system behavior in normal and faulty conditions is the key to modeling for diagnostics.

7.1. Aircraft Model

Let v be the body-axis velocity, ω be the body-axis angular rate, e_3 be a unit vector in the down direction (third column of the rotation matrix from inertial coordinates to body coordinates), and let h be the altitude. Let the inputs consist of a subvector of thrusts, $Thrust \in R^{m_1}$ and a subvector of surface deflection, $\delta \in R^{m_2}$. Let J be the moment of inertia matrix, $mass$ be the mass, S the wing area and $B_{aero} = diag([b, c, b])$ where b is the wingspan and c is the chord.

The corresponding nonlinear aircraft model's states and input vectors are given by:

$$\begin{aligned} x &= [v^T, \omega^T, e_3(\phi,\theta), h]^T \in R^{10} \\ u &= [Thrust^T, \delta^T]^T \in R^m \qquad m = m_1 + m_2. \end{aligned}$$

where ${e_3}^T e_3 = 1$ and

$$e_3 = [\ \ \sin(\theta), \cos(\theta)\sin(\phi), \cos(\theta)\cos(\phi)]^T,$$

$$f_{nom}(x,u) = \begin{bmatrix} \omega \times v + g e_3 \\ J\ {}^1\omega \times J\omega \\ \omega \times e_3 \\ {e_3}^T v \end{bmatrix}$$

$H = g_x H_x$ where

$$g_x = \begin{bmatrix} I_3/mass & 0_{3\times 3} \\ 0_{3\times 3} & J\ {}^1B_{aero} \\ 0_{4\times 3} & 0_{4\times 3} \end{bmatrix}$$

$H_x \in R^{6\times m}$, is a dimensionless coefficient matrix to be identified, and the basis functions, $b(x,u)$, have units of force.

The choice of basis functions for system parameter identification is driven by the fact that the parameters need to be identified very quickly. This does not give us time to move very far in the (x,u) space, so we can only expect to identify a linear (plus bias) approximation of the model. We want to be able to identify the effectiveness of each actuator, so each component of u is a basis function. The only other parameters that are not well known (after failure) are the coefficients that determine the aero forces and moments, which depend on $v \in R^3$, $\omega \in R^3$, and $u \in R^m$. The dependence of the aero forces and torques on $||v||$ is well known, but their dependence on $v/||v||$, and ω may be significantly altered when failure occurs.

If we choose $y = \begin{bmatrix} mass\ v \\ B_{aero}\ {}^1\ J\ \omega \end{bmatrix}$ then

$$C = \begin{bmatrix} mass * I_3 & 0_{3\times 3} & 0_{3\times 4} \\ 0_{3\times 3} & (B_{aero})\ {}^1J & 0_{3\times 4} \end{bmatrix}$$

and we get $C\ g_x = I_6$.

To obtain aero forces and moments that are quadratic in speed, and the dynamic derivatives that are bilinear in v and ω, as well as input terms from thrust and surface deflections, the basis functions are chosen as:

$$b(x,u) = \begin{bmatrix} \frac{1}{2}\rho S||v||^2 \\ \frac{1}{2}\rho S||v||v \\ \frac{1}{2}\rho||v||SB_{aero}\ \omega \\ Thrust \\ \frac{1}{2}\rho S||v||^2\delta \end{bmatrix} \in R^{7+m}$$

.

Let C_f and C_τ be the dimensionless aero-coefficients that determine the forces and torques due to aero-dynamics. Then the coefficient matrix we need to identify is $H_x = \begin{bmatrix} H_v \\ H_\omega \end{bmatrix}$ where:

$$H_v = \left[C_{f_0}(\frac{v}{||v||}, u), \frac{\partial C_f(\frac{v}{\|v\|}, u)}{\partial(\frac{v}{\|v\|})}, C_{f_\omega}, \frac{\partial C_f(\frac{v}{\|v\|}, u)}{\partial u} \right]$$

and

$$H_\omega = \left[C_{\tau_0}(\frac{v}{||v||}, u), \frac{\partial C_\tau(\frac{v}{\|v\|}, u)}{\partial(\frac{v}{\|v\|})}, C_{\tau_\omega}, \frac{\partial C_{\tau_\omega}(\frac{v}{\|v\|}, u)}{\partial u} \right]$$

The individual actuators are represented as third order systems. The torque dynamics are represented by a first order lag and the surface dynamics are represented by a second order system. This lag is connected to the surface dynamics through a switch that has three positions: 1) During normal operation the output of the lag goes through a switch into the surface dynamics. 2) In the case of a stuck surface, a high gain forces the surface position to a stuck position. 3) In the case of a floating surface, no actuator torque is applied to the surface dynamics. Therefore, the floating surface position is driven entirely by the aerodynamic hinge moment.

7.2. Aircraft Parameter Initialization

The basis functions are chosen so that all the aero terms scale with dynamic pressure. To calibrate this system that is quadratic in speed, we need at least two linearizations at two different speeds, since at a single speed, the top four rows of b(x,u) are dependent:

$$\frac{1}{2}\rho S||v|| \begin{bmatrix} ||v|| \\ v \end{bmatrix} = \frac{1}{2}\rho S||v|| \begin{bmatrix} v^T/||v|| \\ I_3 \end{bmatrix} v$$

The only nonzero rows of H are the top 6 rows, so C will be chosen to select all or some of the top six rows. This means that only the top 6 rows of $f_{nom}(x,u)$ need to be computed, so if Euler angles are used instead of the e_3 part of the state, it will not matter. In order to compute H based on linearization data, we need to compute the partial derivative of $f_{nom}(x,u)$ and $b(x,u)$. To simplify the expressions, we will assume that we are trimming about a value of the state that has $\omega = 0$.

$$\frac{\partial f_{nom}}{\partial[x,u]} = \begin{bmatrix} \tilde{\omega} & \tilde{v} & gI_3 & 0_{3\times1} & 0_{3\times m} \\ 0_{3\times3} & 0_{3\times3} & 0_{3\times3} & 0_{3\times1} & 0_{3\times m} \\ 0_{3\times3} & \tilde{e_3} & \tilde{\omega} & 0_{3\times1} & 0_{3\times m} \\ 0_{3\times3} & 0_{3\times3} & e_3^T & 0_{3\times1} & 0_{3\times m} \end{bmatrix}$$

where $\tilde{v}$ is the 3×3 skew sysmetric matrix formed from the elements of v, such that $v \times w = \tilde{v}w$. The $\partial b/\partial[x,u]$ matrix is sparse, with the only non-trivial computations being: $\partial||v||^2/\partial v = 2v^T$ and $\partial(||v||v)/\partial v = ||v||\ [I_3 + (v/||v||)(v/||v||)^T]$

Actually, ρ depends on the state h, but the $\partial b/\partial h$ column of the above matrix will be eliminated anyway by the D matrix. We will choose typically

$$C = \begin{bmatrix} mass * I_3 & 0_{3\times3} & 0_{3\times4} \\ 0_{3\times3} & (B_{aero})^{\ 1}J & 0_{3\times4} \end{bmatrix}$$

which gives $CH = H_x$, or $C = [0_{3\times3}, (B_{aero})^{\ 1}J, 0_{3\times4}]$ if we only want to identify the coefficients associated with the angular dynamics, in the bottom 3 rows of H_x. For the above choice of basis functions, we will choose typically

$$D = \begin{bmatrix} I_7 & 0_{7\times m} \\ 0_{4\times7} & 0_{4\times m} \\ 0_{m\times7} & I_m \end{bmatrix}$$

since the basis functions are only a function of the first six states, $[v,\omega]$, and all the m inputs.

For the first choice of C we get:

$$C[f \quad f_{nom}, \partial f_{nom}/\partial[x,u]] =$$

$$\begin{bmatrix} mass * g * e_3 & mass * \tilde{\omega} & mass * \tilde{v} & 0_{3\times m} \\ 0_{3\times1} & 0_{3\times3} & 0_{3\times3} & 0_{3\times m} \end{bmatrix}$$

This $(7+m)\times(7+m)$ matrix is only rank $6+m$, since its upper 4 rows are only rank 3. The left kernel of the matrix is $[||v||, \quad v^T, 0_{1\times(3+m)}]$. This is due to the fact that the first 4 basis functions are not independent at a single speed. To solve for CH in this quadratic model, we need at least two linearizations $[A,B]_i, (x_{0i}, u_{0i}),\ i = 1,2$. Let $F = [F_1, F_2]$, $G = [G_1, G_2]$. Then the equation for CH is: $F = (CH)G$ and $H_x = C*H = FG^T(GG^T)^{\ 1}$.

The matric, $C_i = C$ scales the first six rows and D selects the first seven and last m columns of the functions, partial derivatives and $[A,B]_i$.

Calibrating Nonlinearities in (α,β):

The basis functions used above were nonlinear in $||v||$ to handle changes in dynamic pressure, but they only captured constant plus linear variation in the unit vector $v/||v||$. To calibrate the coefficients in a larger H matrix that multiplies higher order terms in $v/||v||$, we need to use either time domain data that has large (α,β) excursions, or use multiple linearizations about several (α,β)

points. When using several linearizations, we need to know the mass and moment-of-inertia matrix for each linearization. In this case, we can use a different C_i for each linearization:

$$C_i = \begin{bmatrix} mass_i I_3 & 0_{3\times3} & 0_{3\times4} \\ 0_{3\times3} & (B_{aero})\ {}^1J_i & 0_{3\times4} \end{bmatrix}$$

resulting in linear equations for H_x rather than H, where $H_x = C_i * H$. In the previouse example, the basis functions that depended only on the velocity vector, v, part of the state were: $\bar{q} * S * [1; v/||v||]$, where $v/||v|| = [\cos(\alpha)\cos(\beta), \sin(\beta), \sin(\alpha)\cos(\beta)]^T$, so we capture first-order terms in the unit vector $v/||v||$. To capture the aero functions as arbitrary functions of (α, β), ie for $v/||v||$ anywhere on the unit sphere, we can use spherical harmonics (which are orthonormal if evaluated over the entire 2-sphere) as basis functions. Let $v = [U; V; W]$. Spherical harmonics, truncated to second order, multiplied by $||v||^2$, are:

$$[||v||^2, ||v||v, (5VV \quad 2||v||^2)/3, (10/3)(UU \quad WW),$$

$$(10/3)(2UW), (10/3)(VU), (10/3)(VW)]$$

Four linearizations should be used to calibrate the H matrix that multiplies these second-order terms. For example, linearize about $(\alpha, \beta) = \{(\alpha_0, 0), (\alpha_0+\delta\alpha, 0), (\alpha_0, \delta\beta), (\alpha_0+\delta\alpha, \delta\beta)\}$. Note that if all linearizations are done about $V = 0$ (ie $\beta = 0$), then the $5VV \quad 2||v||^2$ term can be dropped.

7.3. Failure Scenarios

The set of failure scenarios to be addressed will include specific conditions (e.g., aircraft icing, control surface effectiveness degradation, stuck or floating control surface, etc.) that occur often and are amenable to advanced control solutions. We will handle icing conditions and control surface effectiveness degradation by modifying the coefficients in the aerodynamic tables. Individual control surface effectiveness degradation will be implemented by scaling the corresponding column of the surface effectiveness matrix. Unlike the situation with stuck and floating surfaces, control surface effectiveness degradation cannot be detected by fault detection and isolation sensors. Therefore detecting these types of faults requires system identification techniques. Control surface effectiveness degradation faults always cause sudden changes in aerodynamic coefficients, while ice buildup slowly changes aerodynamic coefficients. This has an impact on the identification techniques used. Various identification techniques that will be considered are documented in the bibliography ([3, 5, 7, 14, 4, 6, 15].)

Aircraft performance characteristics are directly dependant on the aerodynamic quantities of the aircraft, especially lift and drag. The loss of performance due to lift and drag degradation and impact of icing on the stability behavior of an airplane observed in some accidents[11, 12] have increased the awareness about the significance of aircraft icing. Studies conducted at the NASA Lewis Research Center have indicated that in icing condition aircraft dynamics experience a decrease in lift and an increase in drag compared to the clean aircraft. These effects could be observed even with the ice protection system activated. Dimensionless stability and control derivatives for the longitudinal flight dynamics of the Twin Otter have been estimated for both clean and iced conditions, and are available in the literature ([13, 2]). It is assumed that icing affected only the derivatives.

7.4. Fault Management Simulation Tests

Active fault management system, uses the aircraft model described in the subsection 7.1, and compares the state derivative of the detection model with the derivative of the states of the actual aircraft. Since we don't have an actual aircraft to work with, we simply compare the detection model with the "truth" model of the aircraft during system performance analysis simulation tests.

The aircraft model could be considered to contain two major parts: the 6-dof aircraft in one part, and the actuator dynamics in the other part. Therefore the detection model is also separated in that way. The 6-dof aircraft model is done in a unified way, using vector notation, while the actuator dynamics are done separately for each of the four actuators. In this paper we will present only results from the simulation that exercises the fault detection, isolation, and accomodation for the 6-dof aircraft, together with the truth model of the aircraft and all actuators. Realistic noise and bias are added to the sensors, and Dryden gust models have been incorporated into the simulation. Gust levels 1, 2, and 3 correspond to a standard deviation of gust magnitude of 0ft/sec, 5ft/sec, and 10ft/sec respectively.

We have a list of faults to choose from, each represented by a different perturbation to the H_x matrix. Each fault introduces a random change in the coefficients in the last 3 rows of the aileron,

elevator and rudder deflection columns of the H_x matrix (Modeling aileron, elevator and rudder effectiveness degradation).

Figure 2 shows results of a Monte-Carlo simulation in which 1000 simulations were run. For testing purposes, we chose a simulation with two successive faults. Fault sizes were randomly varying from 0% to 50% in size, and gust level was 3. Each fault was fault number 4 which denotes perturbing 3×3 block of coefficient matrix H_x that corresponds to $\dot{p}, \dot{q}, \dot{r}$ rows and $\delta_a, \delta_e, \delta_r$ columns. After each fault occurs, a pitch doublet, yaw doublet, roll doublet, and speed step are introduced to give sufficient excitation for I.D. In each case the detection algorithm determined the fault in a timely way and the fault isolation code computed an estimate of the new aero torque coefficients (the bottom half, i.e. the last three rows of the H_x matrix). The least-squares procedure described in earlier sections was used. The controller had a bandwidth of $w_c = 3\frac{rads}{s}$ in the three attitude loops, and a bandwidth of $\lambda_c = .3\frac{rad}{s}$ in the speed loop. The bottom plot on Figure 2 shows the ratio of the time the estimator was on to the total time for fault. The fault size is determined by averaging the size of the change in the perturbed parameters. Some points of interest on these charts are any points that are on either axis. Points on the vertical axis represent false alarms (no fault, but estimator is on), and points on the horizontal axis represent missed detections (there is a fault, but estimator does not turn on). The top plot on Figure 2 shows the amount of time after a fault occurs before the estimator detects the fault. Points that would be on the line 'never turns on' if it were extended are missed detections, and faults that are below the 'never turns on' line on the vertical axis are false alarms. Points on the horizontal axis (delay time = 0) are the result of the second or third fault occurring before the ID signal has completely receded from the previous fault.

To illustrate quality of parameter estimation we show simulation results from a test in which a random fault was introduced to the aileron, elevator and rudder (aileron fault 21.92%, elevator fault 21.15%, rudder fault 31.50%. Simulation results are shown in Figure 3. The detection algorithm determined failure in a timely way. Failure isolation code computed an estimate of the new aero torque coefficients (the last three rows of the H_x matrix coresponding to $\dot{p}$, $\dot{q}$, $\dot{r}$), after the detection algorithm determined that there was a failure. The least-squares procedure described earlier was used and estimation error was smaller than 3.3%.

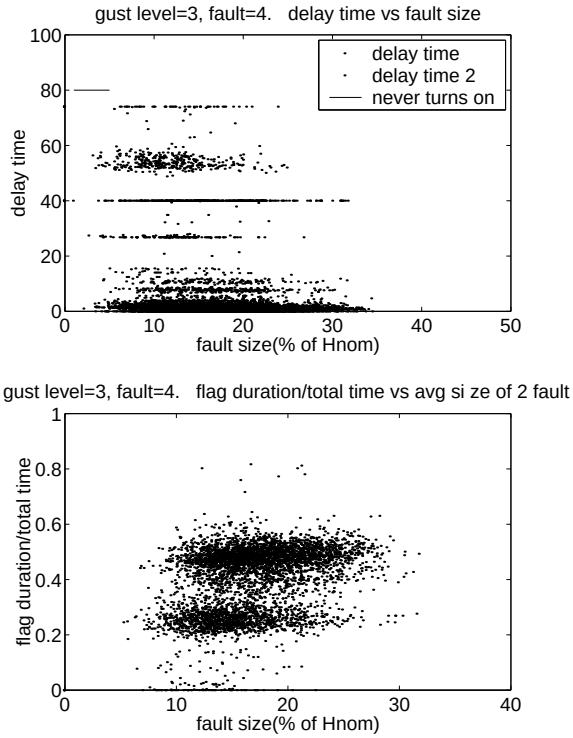

Figure 2: Aircraft FDI Monte-Carlo Simulation

The controller had a bandwidth of $w_c = 3\frac{rads}{s}$ in the three attitude loops, and a bandwidth of $\lambda_c = 0.3\frac{rad}{s}$ in the speed loop. After the fault occurs, a pitch doublet, yaw doublet, roll doublet, and speed step are introduced to give sufficient excitation for ID. Then, the controller reconfigures using the newly identified parameters. The first bars are the original parameter values. The second bars are the damaged values. The third bars are the estimated values.

8. Conclusion

This paper describes the initial phase of development and analysis of an active failure management system for control recovery of commuter and business aircraft. Failure detection algorithms that can reliably detect and isolate system failures with minimal disruption of normal aircraft operations have been developed. To accommodate identified failures wherever possible, autopilot reconfiguration algorithms and pilot cueing strategy have been addressed. Pilot cueing is necessary to inform the pilot of current situation, potential responses, and any autopilot reconfiguration . Preliminary versions of failure management has been implemented for the 6-dof aircraft with promising results.

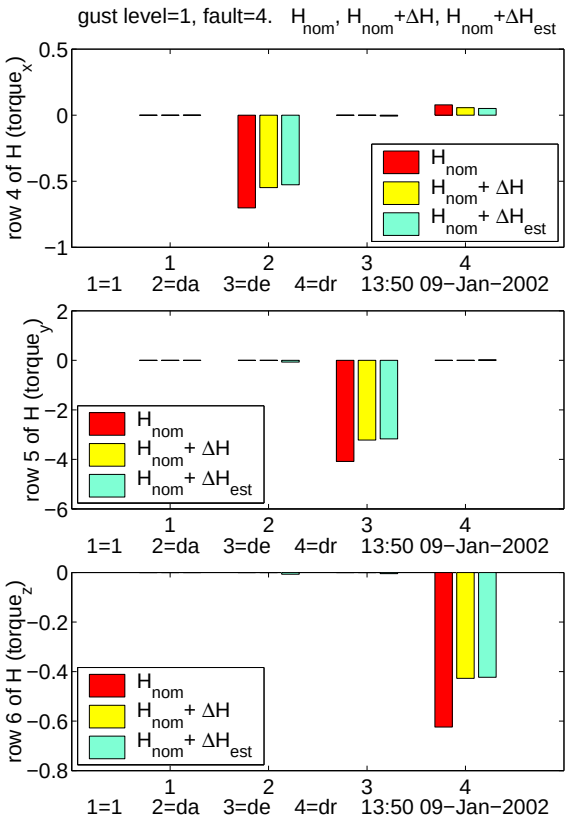

Figure 3: Identified 6-dof coefficients

9. Acknowledgments

Authors would like to thank Tom Bundick, Christine Belcastro, and Celeste Belcastro for many helpful discussions.

References

[1] S. Baker, M. Lamb, G. Li, and R. Dodd. Human factors in crashes of commuter airplanes. *Aviation, Space, and Environmental Medicine*, 1993.

[2] M. B. Bragg, W. R. Perkins, N. B. Sarter, Tamer Basar, P. G. Voulgaris, H. M. Gurbacki, J. W. Melody, and S. A. McCray. An interdisciplinary approach to inflight aircraft icing safety. *AIAA Paper No. 98-0095*, 1998.

[3] P. R. Chandler, M. Pachter, and M. Mears. System identification for adaptive and reconfigurable control. *Journal of Guidance, Control, and Dynamics*, 18:516–524, 1995.

[4] M. Elgersma, D. Enns, S. Shald, and P. Voulgaris. Parameter identification for systems with redundant actuators. *Proceedings of the AIAA Guidance Navigation and Control Conference*, 1998.

[5] G. H. Golub and C. F. Van Loan. *Matrix Computations*. Johns Hopkins University Press, 1996.

[6] S. Van Huffel and J. Vandewalle. The total least squares problem: Computational aspects and analysis. *SIAM*, 1991.

[7] L. Ljung. *System Identification, Theory for the User*. Prentice Hall, 1987.

[8] J. W. Melody, T. Basar, W. R. Perkins, and P. G. Voulgaris. Parameter identification for inflight detection of aircraft icing. *Proceedings of the 14th IFAC World Congress*, 1999.

[9] R. H. Miller and William R. Ribbens. Detection of the loss of elevator effectiveness due to aircraft icing. *AIAA Paper No. 99-0637*, 1999.

[10] K.S. Narendra and J. Balakrishnan. Adaptive control using multiple models. *IEEE Transactions on Automatic Control*, 42:171–187, 1997.

[11] NTSB. *Aircraft accident report, in-flight icing encounter and loss of control Simmons Airlines, d.b.a. American Eagle flight 4184, Avions de Transport (ATR) model 72-212, N401AM, Roselawn, Indiana, October 31, 1994*, volume AAR-96/01. 1996.

[12] NTSB. *Aircraft accident report, in-flight icing encounter and uncontrolled collision with terrain, Comair flight 3272, Embraer EMB-120RT, N265CA, Monroe, Michigan, January 9, 1997*, volume AAR-98/04. 1998.

[13] T. P. Ratvasky and R.J. Ranaudo. Icing effects on aircraft stability and control determined from flight data. *Proceedings of the AIAA Conference*, 1998.

[14] L. Smith, P. R. Chandler, and M. Pachter. Regularization for real-time identification of aircraft parameters. *Proceedings of the AIAA Guidance Navigation and Control Conference*, 1997.

[15] D. G. Ward and R. Barron. A self-designing receding horizon optimal flight controller. 1995.